

Dynamic Optimal Control: A Real-Time Control Optimization Algorithm for Dynamic Networks

Chunyu Pan¹, Zhao Su², Changsheng Zhang¹ and Xizhe Zhang^{2,3*}

1. Northeastern University, Shenyang 110169, China;
2. School of Biomedical Engineering and Informatics, Nanjing Medical University, Nanjing, Jiangsu, 210001, China;
3. Early Intervention Unit, Department of Psychiatry, Affiliated Nanjing Brain Hospital, Nanjing Medical University, Nanjing, China;

*Correspondence: XZ: zhangxizhe@njmu.edu.cn.

Abstract

Real-world complex network systems often experience changes over time, and controlling their state has important applications in various fields. While external control signals can drive static networks to a desired state, dynamic networks have varying topologies that require changes to the driver nodes for maintaining control. Most existing approaches require knowledge of topological changes in advance to compute optimal control schemes. However, obtaining such knowledge can be difficult for many real-world dynamic networks. To address this issue, we propose a novel real-time control optimization algorithm called Dynamic Optimal Control (DOC) that predicts node control importance using historical information to minimize control scheme changes and reduce overall control cost. We design an efficient algorithm that fine-tunes the current control scheme by repairing past maximum matching to respond to changes in the network topology. Our experiments on real and synthetic dynamic networks show that DOC significantly reduces control cost and achieves more stable and focused real-time control schemes compared to traditional algorithms. The proposed algorithm has the potential to provide solutions for real-time control of complex dynamic systems in various fields.

Keyword: Dynamic network; Structural controllability; Control scheme; Driver nodes

1. Introduction

Most complex systems in the real world can be abstracted as complex networks. Controlling these complex networks has important implications for a variety of fields [1-4]. In recent years, the combination of control theory and complex network theory has been applied to a range of areas, including biological networks [5-11], brain networks [12-14], and financial networks [15-19]. A network is controllable if it can be driven from any initial state to a desired state by inputting external control signals [1]. The nodes that receive these signals are called driver nodes [20]. Control signals are inputted at the driver nodes and propagate through the network, changing the state of all nodes in the network. Therefore, finding the appropriate set of driver nodes is crucial for network control.

Networks in the real world are generally dynamic and change over time. For a network, if its topological structure remains relatively stable over a long period of time, we can ignore the influence of the time dimension and approximate it as having a fixed topology, referred to as a static network. For a static network with a fixed topology, the Minimum Driver nodes Set (MDS) can be obtained by finding a maximum matching, as shown in previous work [2], where the set of unmatched nodes is the MDS. This theory has attracted the attention of many researchers and has produced a range of significant results. For example, Ruths [21, 22] have divided the MDS into source nodes, external dilation nodes, and internal dilation nodes to quantify the control structure of a network. Gao [23] and others have proposed the k-walk theory and a framework for analyzing the control of complex networks. Yuan [24] and others have developed a framework for precise controllability on the basis of structural controllability to analyze complex networks with arbitrary structures. Zhang et al. [25-28] suggested using preferential matching to find MDS with characteristic properties and also proposed that reversing or removing the edges can change the control mode of the network.

However, in many real-world networks, the topological structure tends to change frequently over time. For such dynamic networks, the changes in topology over time cannot be ignored. For example, the average similarity in topological structure of the dynamic network *CollegeMsg* [29] is only 8%. Therefore, for a dynamic network, a MDS based on a single snapshot of the static topology at a given time may no longer be effective at other times [28]. Thus, for networks with topologies that change over time, we must design new methods to compute dynamic control schemes that adapt to these changes.

For a dynamic network G , it can often be treated as an ordered sequence of static networks, known as a temporal network [30, 31], where G_t is the static network at time t and the topological structure of G_t is formed by all the edges that occur over a period of time. A straightforward idea to continuously control such temporal networks is to compute MDS for each network G_t corresponding to time t . However, the drawback of this approach is that independently computing MDS for each time-specific network may result in large discrepancies between MDSs at different times, leading to higher control costs. Therefore, some works [32-34] have attempted to use optimization algorithms to compute control schemes for multiple times in a network. For example, Posfai et.al proposed that the maximum controllable subspace of each driver node can be determined by its number of independent paths [33]; Ravandi et.al designed a heuristic algorithm based on independent paths and determined the approximate minimum number of driver nodes required to control a known temporal network [34]. However, the above methods assume that the topological structure change of time varying network is known, and thus the optimal control scheme for this period of time can be calculated. However, when a dynamic network encounters unknown changes, these methods still have to recalculate control schemes, which leads to higher control costs.

For most real-time dynamic networks, it is difficult to know in advance the changes in the network's topology. How to give an optimal control scheme for the network under the premise of continuous topological changes is still an open problem to date, as far as we know. The difficulty of this problem lies in two aspects. On the one hand, it is costly to recalculate the control scheme of the entire network when the topology changes frequently. One of the challenges is how to use the existing control scheme of the network to quickly calculate the

control scheme after the topology changes. On the other hand, in order to maintain real-time control of the dynamic network, we need to calculate the MDS corresponding to each time. How to minimize the changes in these MDSs over time, thereby obtaining the minimum overall control cost, is another challenge that needs to be addressed.

Figure 1 gives an example of a dynamic network G . Let the current time be t_n , the topology of all subgraphs before time t_n is known and the optimization control scheme C_n of these networks can be calculated using existing methods. However, as the network changes to the next time t_{n+1} , it is possible that the new network topology G_{n+1} may not be controlled by C_n . This means that when the network changes in real time, the control scheme needs to be dynamically adjusted to maintain control of the dynamic network. If the network's control scheme is recalculated based on the maximum matching, the new control scheme may differ significantly from the original, thereby increasing the control cost. On the other hand, since the network needs to be continuously controlled, we need to calculate the control scheme corresponding to each future time for the network. Therefore, when the network's topology changes continuously over time, the total sum of all control schemes required to control the network may be much larger than the MDS at a single time.

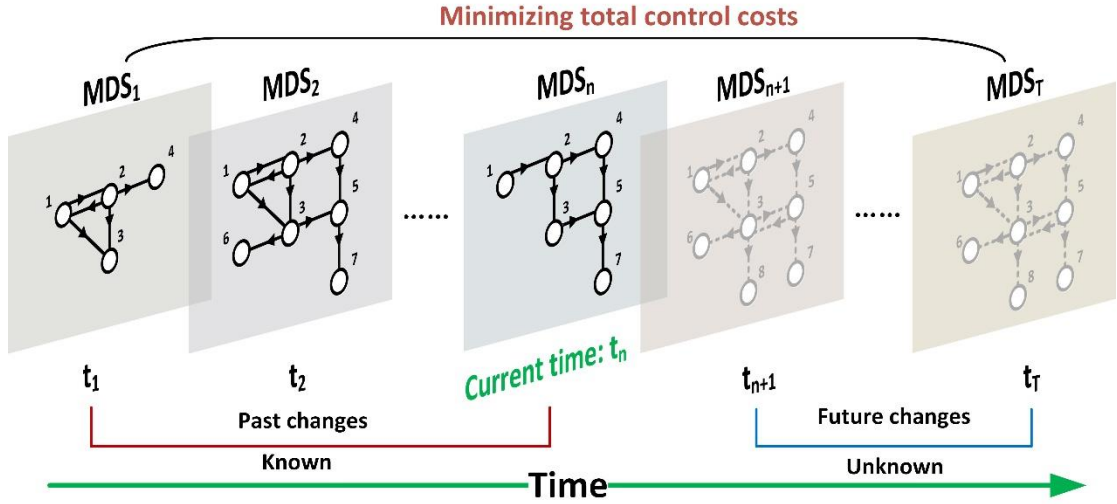


Figure 1. Real-time control of dynamic networks. In real-time control, for the current time t_n , the current and previous network topologies $[G_1, G_n]$ are known, while the future network topologies $[G_{n+1}, G_T]$ are unknown. For the unknown network, we need to continuously calculate its control scheme and minimize the overall control cost.

The problem of selecting an appropriate Minimum Driver nodes Set (MDS) for a temporal subgraph of a network can be addressed by considering the similarity of the current MDS to a previous one, while taking into account the future stability of the selected MDS. However, computing all MDS for a network is a #P hard problem [35]. To address this issue, our prior work proposed an input graph theory [36] that represents the relationship between all MDS in a network, and provided an algorithm for enumerating all the driver nodes in MDS [37] which can be used to guide the selection of the current MDS of the network. Furthermore, we have developed a network structure-based node stability evaluation method that can identify a suitable set of nodes to serve as the current MDS, taking into account not only the similarity with the previous MDS but also the future stability of the selected MDS.

In summary, this study proposes a new approach, dynamic optimal control (DOC), for addressing the real-time control problem in dynamic networks. The algorithm aims to minimize the overall cost of controlling the dynamic network by selecting appropriate Minimum Driver nodes Set (MDS) from the set of all possible MDS of the current subgraph. This reduces the difference between the current MDS and the previous MDS, and subsequently minimizes the overall control cost of the dynamic network. To achieve this, we have designed a node importance evaluation method that is suitable for control of dynamic networks. This method ranks nodes based on their topological stability and the likelihood of being a driver node, thus guiding the selection of the current MDS. Additionally, we have also developed a partial matching-based maximum matching repair method that allows us to quickly calculate the current time network's MDS based on the topological changes of the current time network and the previous network's MDS. Furthermore, the proposed algorithm can be applied to various types of dynamic networks, such as transportation networks, communication networks, and social networks. It can also be used for various control tasks, such as fault diagnosis, network reconfiguration, and traffic control. The proposed algorithm provides a new perspective on real-time control of dynamic networks and can be applied to various fields.

2. Controllability of real-time dynamic network

A real-time dynamic network G is defined as a network whose topology changes over time. For the networks that the dynamical processes can be decoupled [31], by setting duration time τ , $\tau \in \mathbb{Z}$, a real-time dynamic network $G = \{G_1(V_1, E_1), G_2(V_2, E_2), \dots, G_T(V_T, E_T), \dots\}$ can be represented as a sequence of snapshots [38]. We assume that the system spends a finite amount of time in each snapshot [39, 40], hence the Zeno phenomenon [41, 42], of infinitely fast switching, is unlikely to occur in real-time dynamic networks [30]. In a snapshot that exists in the time interval $[t, t + \tau)$, $t \in \mathbb{N}$, we consider it as a static temporal subgraph $G_t(V_t, E_t)$ in time point t , where $V_t = \{v_1, v_2, \dots, v_N\}$ and $E_t = \{e_1, e_2, \dots, e_L\}$ represent the set of nodes and edges that appearing in the time interval $[t, t + \tau)$. For the current time point t_n , only the temporal subgraph $G_\varepsilon(V_\varepsilon, E_\varepsilon)$, $\varepsilon \in [1, n]$ is known and subsequent network topology changes are unknown (Figure 1).

A dynamic network can be considered as a linear time-variant (LTV) system and the dynamics of the system can be represented as [20, 43],

$$\frac{dx(t)}{dt} = A(t)x(t) + B(t)u(t)$$

where vector $x(t) = (x_1(t), \dots, x_N(t))^T$ represents the system state vector of N nodes at moment t . The matrix $A(t)$ is a state parameter describing the components of the dynamic network at moment t . The matrix $B(t)$ of $N * M$ ($M \leq N$) is the input matrix from which the controlled node is identified by the external controller at moment t . Vector $u(t) = (u_1(t), \dots, u_M(t))^T$ represents the input vector of M nodes at the moment t . The controller uses input vector $u(t)$ to control the entire system and a single control signal $u_i(t)$ can typically drive multiple nodes. For a dynamic network G which the dynamical processes can be decoupled [31], it can be represented as a sequence of static networks, $G = \{G_1(V_1, E_1), G_2(V_2, E_2), \dots, G_T(V_T, E_T), \dots\}$, which we called as temporal subgraphs. Therefore,

the temporal subgraph G_i is governed by the canonical linear time-invariant (LTI) dynamics [30]

$$\frac{dx(t)}{dt} = A_i x(t) + B_i u(t)$$

In contrast to LTV dynamics, the matrices $A(t)$ and $B(t)$ of the temporal subgraph G_i are constrained to the matrix A_i and B_i which is the same as the static network.

According to the Kalman rank condition [1], G_i is controllable if and only if the matrix $C = (B, AB, A^2B, \dots, A^{N-1}B)$ is full rank, and the system can be driven from any initial state to any final state in a finite time. However, for most real networks, it is extremely difficult to obtain the specific weights for each edge. Lin [2, 44] proposed structural controllability to assess the ability to control a system based on its underlying structure, rather than its detailed equations. The concept of structural controllability is based on graph theory, and it provides a way to determine the minimum number of inputs that are required to control a system, and to identify the optimal locations to place these inputs.

The minimum set of driver nodes in a network, also known as the MDS, plays a critical role in determining the structural controllability of the network. The MDS represents the smallest set of nodes that need to be controlled in order to drive the entire network to a desired state. The computation of the MDS is achieved by finding the maximum matching in the underlying graph representation of the network [2]. A matching in a network refers to an edge set that does not share nodes in common. The maximum matching is the matching with the largest number of edges, and it can be found by using the Hopcroft-Karp (HK) algorithm [45]. Once the maximum matching is found, the nodes that do not have any directly pointed matched edges are considered to be the driver nodes [2]. The identification of the MDS allows for the efficient control of the network, as only a small number of nodes need to be manipulated in order to drive the entire network to a desired state.

However, the maximum matching and subsequently, the MDS are not unique in most networks [46, 47]. There may be multiple MDSs that offer the same level of control for a given network. The specific set of driver nodes can vary depending on the requirements and objectives of the control problem. This flexibility allows for a more customized and efficient control design, tailored to the specific needs of the network. For example, Figure 2 demonstrates a network with three MDSs, each composed of different driver nodes. Despite the differences in the specific driver nodes, each of these MDSs can achieve the same level of controllability in the network. In practical applications, the choice of the MDS can be made based on the specific requirements of the control problem, allowing for a more customized and efficient control design.

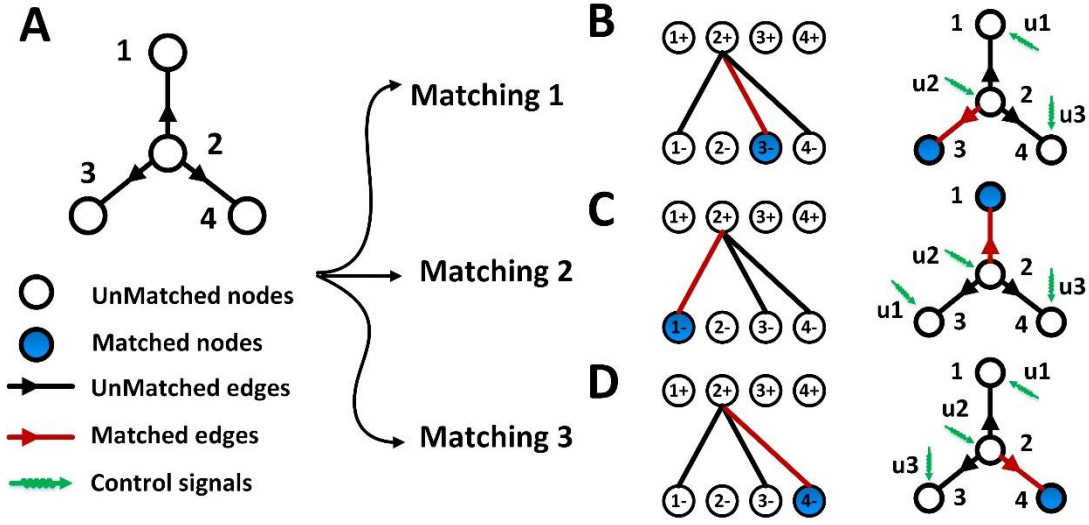


Figure 2. A simple network with three different MDS.

3. Real-time control for dynamic network

3.1 Motivation

In this section, we consider the problem of real-time control for dynamic networks. The real-time control refers to the ability to control a dynamic network in real-time, meaning that the MDS need to be recalculated to maintain full control when the network is changing. This is a challenging task as it requires the ability to predict the structure of the network in real-time, and then apply appropriate MDS to current temporal graph to ensure the control of the network.

For a dynamic network, each individual temporal subgraph possesses its unique MDS. To effectively control dynamic network, it is necessary to identify the optimal combination of driver nodes that minimizes the cumulative change in MDS over all temporal subgraphs. It is crucial to consider the network's dynamic nature and its evolution over time while striving to find the most efficient control strategy that requires the least number of driver nodes. It should be noted that each temporal subgraph usually contains multiple MDSs consisting of different driver nodes. Therefore, to achieve an optimal solution, we need to select similar MDSs across adjacent temporal subgraphs to ensure consistent and minimal control effort.

For instance, Figure 3B depicts an example of a dynamic network where the MDS at time t_1 comprises nodes 1 and 2. The network undergoes changes at t_2 , leading to the MDS being node 3 and 4. As time progresses, the MDSs may continue to change, leading to an increase in the overall control cost of the dynamic network. In the illustrated example, the dynamic network comprises five temporal subgraphs, with each subgraph exhibiting a maximum of three driver nodes. However, due to the variations in the MDS over time, it is necessary to control a cumulative total of eight driver nodes, with nine changes in driver nodes observed between neighboring temporal subgraphs.

An effective approach for selecting the MDS for current temporal graph is to take into account both historical and future structural information of the network. With respect to historical information, the aim is to maintain consistency with previous MDSs by making the

current MDS as similar as possible to them, thereby reducing changes in the MDS. Furthermore, it is also important to anticipate future changes in the network, such that the current MDS is subject to minimal changes in the future. To achieve this goal, the selection of stable nodes as driver nodes of the current MDS can be employed, which will result in reduced future changes to the MDS. As an example, in the same sample as Figure 3B, Figure 3C only shows the accumulation of four driver nodes and only two changes in the driver nodes between neighboring temporal subgraphs.

Overall, when controlling dynamic networks in real time, the selection of the MDS at each temporal graph should be guided by two principles. The first principle is based on historical information and aims to ensure consistency with previous MDSs. The second principle is focused on future considerations and involves the selection of nodes with better stability as the MDS driver nodes, to minimize future changes to the MDS. Consequently, we will design a MDS calculation algorithm that takes into account the nodes importance for control to choose the appropriate driver nodes as the MDS. This approach will minimize the variations in the overall MDS of the dynamic network and reduce the control cost.

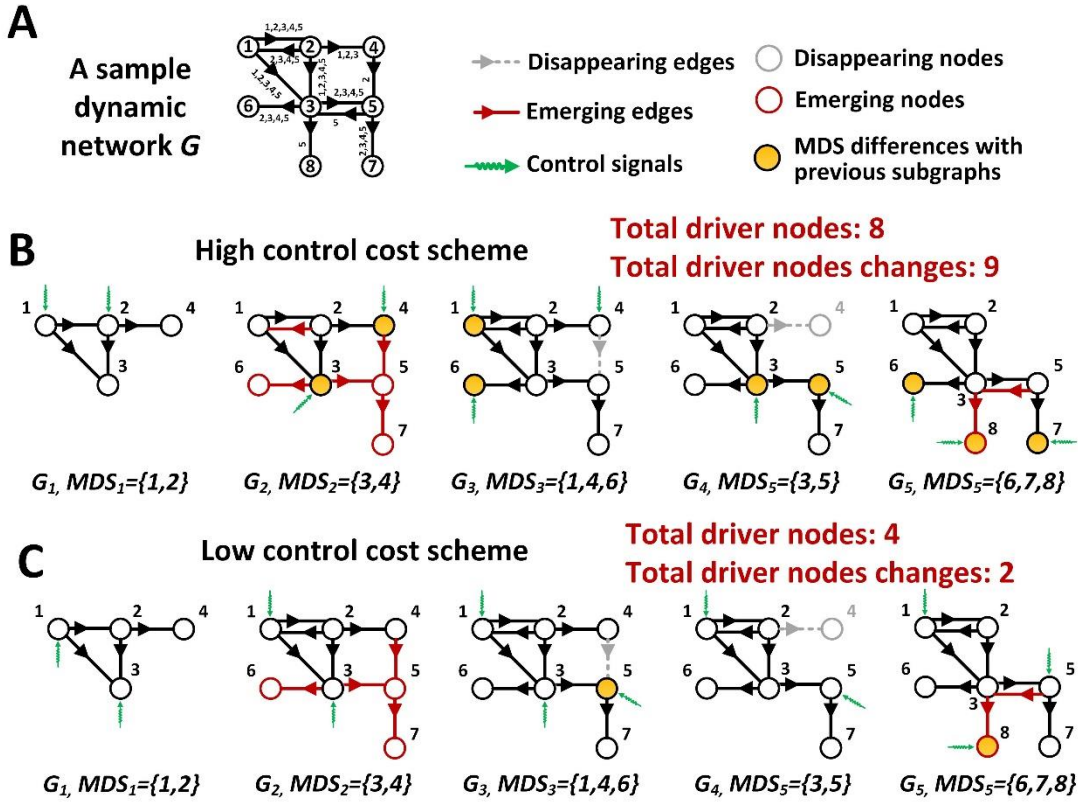


Figure 3. Different control schemes of a dynamic network. **(A)** A sample dynamic with five temporal subgraphs. **(B)** A control scheme with a high control cost, where eight driver nodes are required for all five temporal graphs and there are nine changes in driver nodes between neighboring temporal subgraphs; **(C)** A control scheme with a low control cost, where the total number of driver nodes is four and there are only two changes in the driver nodes between neighboring temporal subgraphs.

3.2 Algorithm

To obtain the MDS that can reduce the overall control cost of the network, we have designed an algorithm to measure the importance of nodes while considering both historical information of the network and future changes. This algorithm performs a ranking of the nodes in the current temporal subgraph based on the calculated importance. The resulting MDS is then composed of the expected nodes, thereby reducing the overall control cost.

For the importance of nodes, we consider that nodes that are stably present in the network should be prioritized. To measure the stability of a node v , we take two aspects into account: 1) the number of edges that node v has in the temporal subgraphs, i.e., the degree of node v ; 2) the similarity of edges that node v has in adjacent temporal subgraphs. A high degree means that the node interacts with more other nodes in the network, making it more stable [48, 49]. On the other hand, a low-degree node can also be stable if its edges never change [50]. Therefore, we calculate the similarity of edges that node v has in neighboring temporal subgraphs, i.e.,

$$S_t(v) = \frac{|E_t(v) \cap E_{t-1}(v)|}{|E_t(v) \cup E_{t-1}(v)|}, \text{ where } E_t(v) \text{ denotes the edge set of node } v \text{ in temporal subgraph } G_t.$$

The higher the edge similarity of node v , the more stable the node is considered to be. Furthermore, as network changes are a continuous process, we need to consider the stability of node v over a certain period of time. Therefore, we take the sum stability of node v in the previous l subgraphs, i.e., $[G_{i-l}, G_i]$, as the value of its stability. To sum up, for node v in the current temporal subgraph G_i , its stability $\sigma_i(v)$ can be expressed by the following formula (1).

$$\sigma_i(v) = \sum_{t=i-l}^i \left(\frac{|E_t(v) \cap E_{t-1}(v)|}{|E_t(v) \cup E_{t-1}(v)|} * \frac{\sum_j x_{v,j}(t)}{N(t)-1} \right) \quad (1)$$

where l is the number of preceding temporal subgraphs that need to be calculated, $E_t(v)$ represents the edge set of node v in the temporal subgraph G_i , $\frac{|E_t(v) \cap E_{t-1}(v)|}{|E_t(v) \cup E_{t-1}(v)|} \in [0,1]$ is the edge similarity of node v in adjacent subgraphs; $\frac{\sum_j x_{v,j}(t)}{N(t)-1} \in [0,2]$ is the degree centrality of node v at the current time, where $N(t)$ is the number of nodes in the current temporal subgraph. Due to being a directed network, the bidirectional edges are counted twice, thus the range of degree centrality is $[0, 2]$.

To reduce the difference with the MDS of previous subgraph, it is necessary to consider selecting the driver nodes in the previous MDS as the driver nodes of the current subgraph. Thus, the node importance metric of current temporal subgraph G_i is given:

$$q_v = 2l * MDS_{i-1}(v) + \sigma_i(v) \quad (2)$$

where $MDS_{i-1}(v)$ represent whether the node appeared in the previous MDS, which can be either 1 if the node appears in the previous MDS or 0 if it does not:

$$MDS_{i-1}(v) = \begin{cases} 1, & v \in MDS_{i-1} \\ 0, & v \notin MDS_{i-1} \end{cases} \quad (3)$$

It should be noted that the above node importance metric has the following property:

Property 1: Consider a temporal subgraph G_i of a dynamic network G at time i , for two nodes v_1 and v_2 in G_i , if $v_1 \in MDS_{i-1}$ and $v_2 \notin MDS_{i-1}$, then $q_{v_1} > q_{v_2}$.

Proof: For a non-fully connected temporal subgraph G_i , since $S_i(v) = \frac{|E_t(v) \cap E_{t-1}(v)|}{|E_t(v) \cup E_{t-1}(v)|} \in [0,1]$

and $\frac{\sum_j x_{v,j}(t)}{N(t)-1} \in [0,2)$, then $\sigma_i(v) = \sum_{t=i-1}^i (\frac{|E_t(v) \cap E_{t-1}(v)|}{|E_t(v) \cup E_{t-1}(v)|} * \frac{\sum_j x_{v,j}(t)}{N(t)-1}) \in [0,2l)$. According to formula (2) and (3), for the node v_1 that appears in MDS_{i-1} , $2l * MDS_{i-1}(v_1) = 2l$, then $q_{v_1} \in [2l, 4l)$. For the node v_2 that not appears in MDS_{i-1} , $2l * MDS_{i-1}(v_1) = 0$, then $q_{v_2} \in [0, 2l)$. In conclusion, $\max(q_{v_2}) < \min(q_{v_1})$, then $q_{v_1} > q_{v_2}$ is established, proof complete.

According to property 1, if a node was a driver node in the previous subgraph, it should also be prioritized as a driver node in the current subgraph. Based on this property, we will sort nodes according to their importance and select an appropriate MDS for the current subgraph.

A network usually has multiple distinct MDSs [46, 47], therefore, an appropriate MDS can be selected according to different requirements. A straightforward idea is to calculate all MDSs in a static network and then select an appropriate one. However, calculating all MDSs is a #P-hard problem, which is unfeasible in large networks [35]. Our previous work [25, 26] provides a preferential matching algorithm, which obtain the MDSs based on node preferences.

However, the preference matching algorithm still requires multiple calculations of maximum matchings, resulting in a higher complexity. To address this issue, we propose a new algorithm specifically designed for dynamic networks, which can obtain an MDS satisfying the node preference sequence with only one calculation of maximum matching. The algorithm is based on the maximum matching of the pre-sequence temporal subgraphs and starts from the changed nodes in the current network to repair the damaged maximum matching due to network topology changes, thereby obtaining a new MDS. In this process, we will use the sorted node importance to guide the search process of the algorithm and obtain an MDS satisfying the node constraints.

The basic idea of the Maximum Matching algorithm is as follows: First, for the currently unmatched nodes in the current matching M (initially $M = \emptyset$), find their augmenting path. Second, obtain a new matching M' based on the augmenting path, and let $M = M'$. Repeat this process until no augmenting path exists, and ultimately the maximum matching M^* of the network can be obtained, and all the unmatched nodes will form the MDS of the network. During this process, the order of node search when the unmatched node is searching for the augmenting path will result in different MDS [26] (Figure 2). Therefore, if we can search for the augmenting path in accordance with a specific node order, we can obtain an MDS with a certain specific attribute. We introduce the node weight q into the search process of the augmenting path. Specifically, the algorithm first finds all the unmatched nodes in the current matching M , then searches for the augmenting path according to the ascending order of the weight q (Figure 4.B), calculates the new matching M' , and sets $M = M'$. Repeat this process until no new augmenting path is found, at which point the matching M is the maximum matching M^* of the network (ALGORITHM 1). This process will make the nodes with smaller weights complete the search first, while the nodes with larger weights will eventually become the driver nodes because they are unmatched. The pseudo-code for the DOC algorithm is presented as ALGORITHM 1.

Figure 4 provides a demonstration of the algorithm's operation with parameter $l = 1$. Initially, in temporal subgraph G_1 , the weights $\{q_1 = 0, q_2 = 0, q_3 = 0, q_4 = 0\}$ are calculated using the method outlined in formula (2), resulting in an MDS of $\{3, 4\}$. Subsequently, when the network evolves from G_1 to G_2 , the node weight q is recalculated using formula (2), and an augmenting path search is performed by prioritizing the weights in descending order, leading to an MDS of $\{3, 4\}$ (as seen in Figure 4A). This procedure is repeated until the network no longer undergoes any changes. To illustrate the matching process in detail, we use the network topology present at G_2 (shown in Figure 4B). Initially, all nodes are deemed unmatched nodes in the bipartite graph b_0 , and the node search order is set to $\{7, 6, 5, 1, 2, 4, 3\}$. Next, the augmenting path of node 7 is searched for, resulting in b_1 . This is followed by the search for the augmenting path of node 6, resulting in b_2 . Subsequently, the search for the augmenting path of node 5 is skipped, as it has already been matched in the previous step, and the process proceeds to node 1, resulting in b_3 . This process continues until the augmenting path search is complete, yielding the final result depicted in b_4 . As a result, the unmatched nodes $\{3, 4\}$ are determined to be the MDS of the temporal subgraph G_2 .

ALGORITHM 1: Dynamic Optimal Control

1. **Input:** dynamic network G ; parameter l
 2. **Output:** control scheme cs ;
 3. **Initial** control scheme cs ; weight vector q ; subgraph index t ; previous matching M' ; degree centrality list $DClist$; edge similarity list $ESlist$; previous subgraph G_p ; previous MDS MDS_p ;
 4. **Repeat**
 5. $t++$;
 6. **Get** current temporal subgraph G_t ;
 7. **Update** $DClist$ by subgraph G_t ;
 8. **Update** $ESlist$ by subgraph G_t and G_p ;
 9. **Update** vector q by $DClist$, $ESlist$, MDS_p and l ;
 10. $MDS_t, M^* = \text{AugmentingPathSearch}(G_t, q, M')$;
 11. **Add** MDS_t into control scheme cs ;
 12. **Let** $M' = M^*$;
 13. **Let** $G_p = G_t$;
 14. **Let** $MDS_p = MDS_t$;
 15. **Until** the network no longer changing;
 16. **Return** control scheme cs ;
 - 17.
 18. **Function** $\text{AugmentingPathSearch}(G_t, q, M')$
 19. **Initial** matching $M = \text{previous matching } M'$; $MDS = \text{null}$;
 20. **Get** order q' by ascending weight vector q ;
 21. **Repeat**
 22. **Initial** MDS ;
 23. **Get** unmatched nodes set un by matching M ;
 24. **For** node n **in** un **by** order q' :
 25. **If** node n has the augmenting paths **then**:
 26. Expand the augmenting paths and obtain a new matching M^* ;
 27. **Let** $M = M^*$;
 28. **Find** all unmatched nodes un' after matching;
-

-
29. **Let** $MDS = un'$
 30. **Until** no augmenting path is found;
 31. **Return** $MDS; M^*$;
-

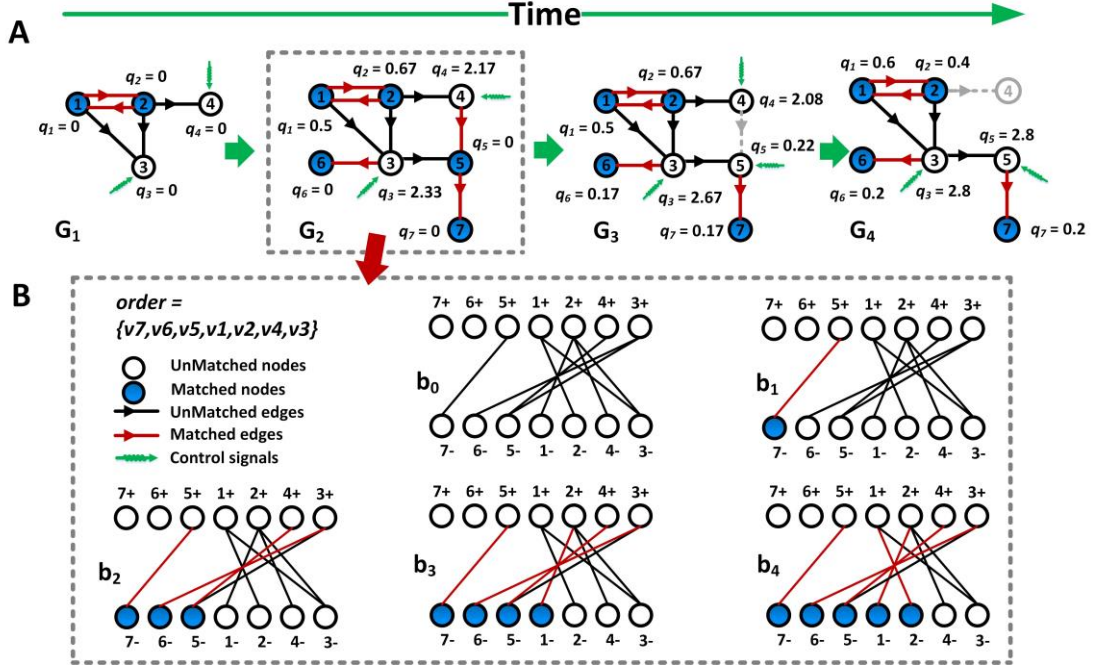


Figure 4. A DOC algorithm instance. (A) A simple dynamic network with 4 temporal subgraphs. (B) The process of compute maximum matching of G_2 .

4. Results

4.1 Datasets and performance metric

We first evaluate the performance of our algorithm on synthetic networks. We constructed multiple dynamic networks based on the Erdős-Rényi (ER) random networks model [51]. The network construction process is as follows: first, we generated a number of ER network instances as the initial network, all of which have $N=10,000$ nodes, with an average degree range of 2.0-8.0 and a step size of 0.2. We then randomly reconnected a portion of the edges with an edge reconnection ratio of r . For each random network instance, we randomly reconnected 99 times, and finally obtained 100 temporal subgraphs, which were used to simulate the dynamic changes of the network. The reconnection ratio r ranges from 0.01-0.30 with a step size of 0.01, i.e., each network instance generates 30 dynamic networks with different change rates, and a total of 930 dynamic networks are generated.

We conducted further evaluations of our algorithm on 20 real-world dynamic networks, including email, human contact, and hospital-ward networks, which were selected from

previous studies [29, 52, 53]. These networks possess more complex topologies and dynamic structures compared to those generated by the ER random network model. Therefore, their temporal subgraphs are expected to exhibit stronger evolutionary patterns, which allows for a more accurate assessment of the DOC algorithm's performance. The raw data of these dynamic networks contained information on the start nodes, end nodes, and timestamps of each edge in the network. To prepare the data for analysis, we divided each network into multiple temporal subgraphs. This was accomplished by setting $T_n = T_{n-1} + \tau$, where τ is the length of the timestamp segmentation and T_0 is the minimum timestamp T_{min} of the network. We then saved the edges with timestamps within the range $[T_{n-1}, T_n]$ as the temporal subgraph G_n of the network. Detailed information on the 20 real networks used in this study is provided in Table 1.

To evaluate the performance of the proposed algorithm, two performance metrics have been devised. The control cost of the dynamic network is quantified through the computation of the union of all temporal subgraph's MDS, represented by $UMDS = \bigcup_{i=1}^T MDS_i$, where T denotes the total number of temporal subgraphs. The UMDS represents the total control cost of the dynamic network, with a lower value indicative of a more efficient control. Additionally, the frequent fluctuations in the MDS of continuous temporal graphs may result in a high control cost, even with a low overall UMDS. To address this issue, we have also calculated the difference between consecutive temporal graph MDS, represented by $ECC = \sum_T |MDS_i - MDS_{i-1}|$. This metric represents the number of driver nodes that belong to the current MDS but are not present in the previous one, allowing us to monitor the stability of the control process.

We opted for the Maximum Matching (MM) algorithm proposed by Liu et al [2] as our comparison algorithm. This is because other previous algorithms [32-34] focused on finding the minimum UMDS for dynamic networks with non-real-time control using post-hoc analysis, and they ignored the problem of driver node changes in real-time control, i.e., ECC. As a result, they failed to provide the MDS for controlling each temporal subgraph. The MM algorithm is a classic algorithm for computing the MDS of a static network and uses the Hopcroft-Karp maximum matching algorithm [45] to obtain the maximum matching and therefore the MDS. We applied both the DOC algorithm and the MM algorithm to calculate the MDS for each temporal graph of the dynamic network and then aggregated them to obtain the UMDS and ECC of the dynamic network. The experimental results will compare the sizes of UMDS and ECC between the two algorithms, demonstrating the superior performance of our algorithm.

4.2 Results of synthetic dynamic networks

The results of the DOC and MM algorithms on synthetic networks are presented in Figure 5. Our findings indicate that the DOC algorithm has a lower ECC than the MM algorithm for all networks (Figure 5A, where $ECC_{DOC}/ECC_{MM} < 1.00$) and has a lower UMDS in over 99.89% of the network (Figure 5B, where $UMDS_{DOC}/UMDS_{MM} < 1.00$). The result implying that the control schemes computed by the DOC algorithm have lower control costs compared to those computed by the MM algorithm. Additionally, for networks with the same average degree k , the optimization performance of the DOC algorithm decreases and becomes closer to the results of the MM algorithm as the rate of change r increases. This suggests that the performance of the DOC algorithm declines when the network experiences significant changes. Nevertheless,

for vast most networks, regardless of the extent of changes in the network topology, the DOC algorithm outperforms the MM algorithm.

In order to gain a deeper understanding of the performance of the DOC algorithm, we conducted a detailed analysis of the results of each temporal subgraph in dynamic networks (Figure 5D). For each temporal subgraph, we compared the size of the ECC obtained from the MM algorithm and the DOC algorithm. Our findings show that when the average degree $k < 4$, the DOC algorithm outperforms the MM algorithm in almost all of the temporal graphs. However, when the average degree $k > 4$, the proportion of instances where DOC and MM perform equally increases significantly (Figure 5D). This phenomenon can be attributed to the improvement of network connectivity as the average degree k increases, leading to a rapid decrease in the size of the MDS of the network (Figure 5C), i.e., the number of driver nodes required to control the network decreases significantly. This results in a smaller optimization space for the MDS of each temporal graph, leading to a large number of identical results, ultimately causing a decline in overall optimization performance (Figure 5A, the mean value of ECC_{DOC}/ECC_{MM} is 0.631 when $k=2.0$ and the mean value of ECC_{DOC}/ECC_{MM} is 0.841 when $k=8.0$).

In addition, according to the formula (2), we analyzed the impact of the number of preceding temporal subgraphs l on the optimization results. We calculated the results of the DOC algorithm for four different cases: $l=1, 5, 10$ and *all*. The results indicated that the different values of the parameter l had no significant impact on the final optimization results (Figure 5, 6 and 7).

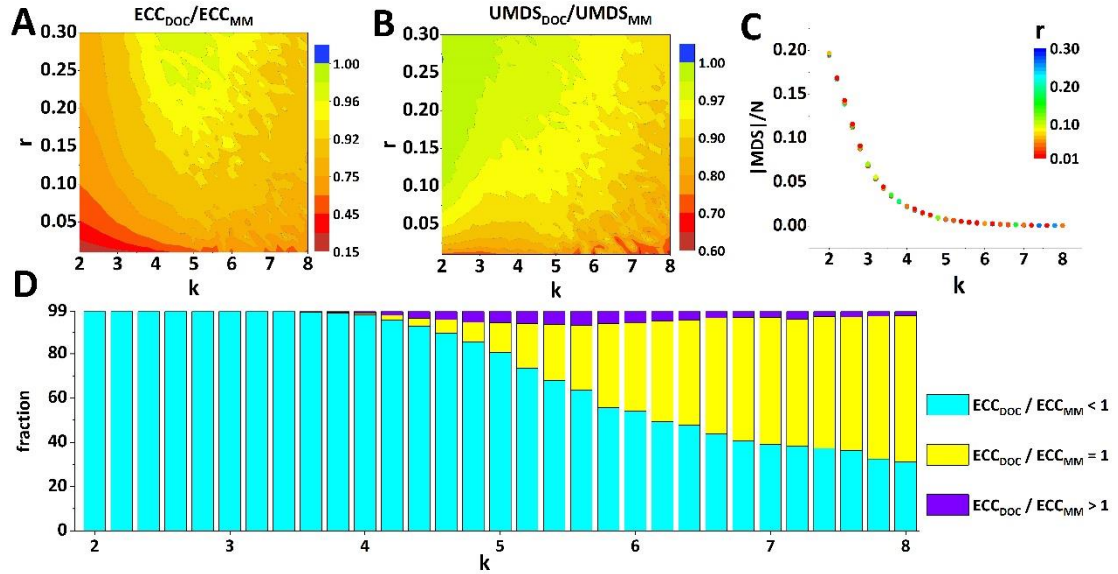


Figure 5 Illustrates the performance of our DOC algorithm compared to the MM algorithm on synthetic networks with $l=5$. **A.** the comparison of the ECC of the two algorithms, where the horizontal axis denotes the average degree k of the network and the vertical axis represents the change rate r . The color scale indicates the value of the ratio ECC_{DOC}/ECC_{MM} ; **B.** the comparison of the UMDS obtained by DOC and MM algorithms; **C.** the relationship between the MDS size and the average degree of the network. The horizontal axis represents the average MDS size across all temporal subgraphs, while the vertical axis shows the average degree k ; **D.** the performance of the DOC algorithm on individual temporal subgraphs for a given average

degree k , where the fraction is computed based on the average of all temporal subgraphs with different change rates r .

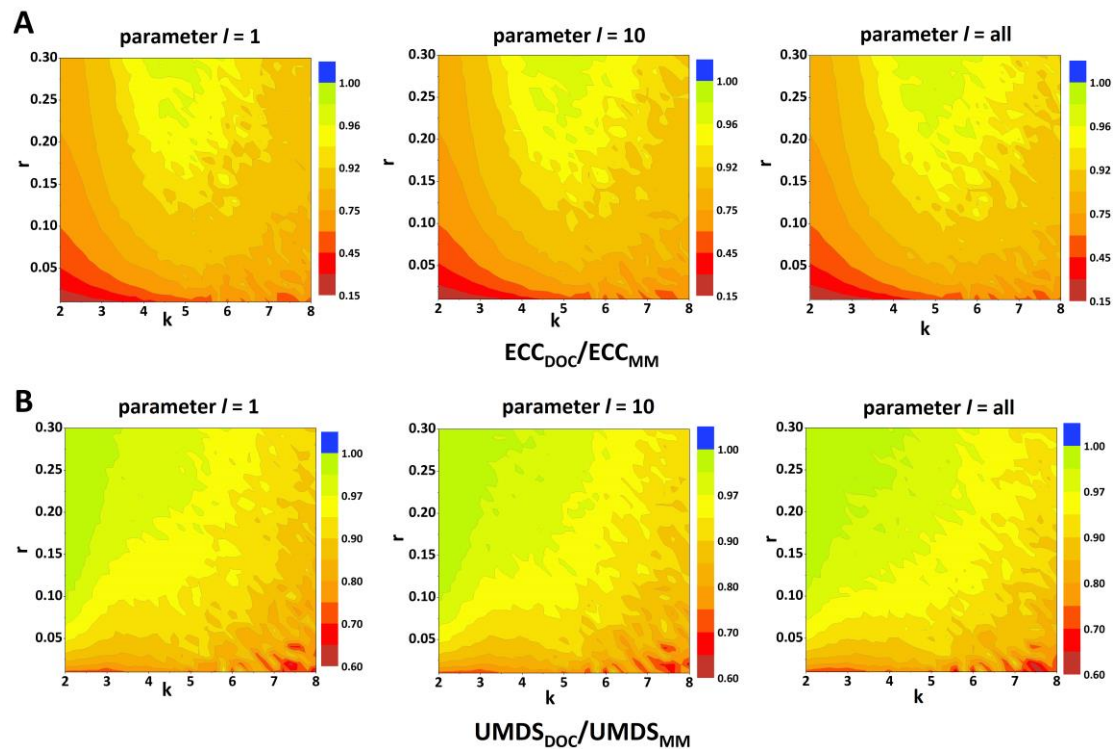


Figure 6. The results of DOC algorithm performance on synthetic networks with different $l=1, 10$ and *all*. (A) The comparison of ECC in DOC and MM algorithms when $l=1, 10$ and *all*. The horizontal axis represents the average degree k of the network and the vertical axis represents the change rate r . The color scale indicates the value of the ratio ECC_{DOC}/ECC_{MM} ; (B) The comparison of of UMDS in DOC and MM algorithms when $l=1, 10$ and *all*.

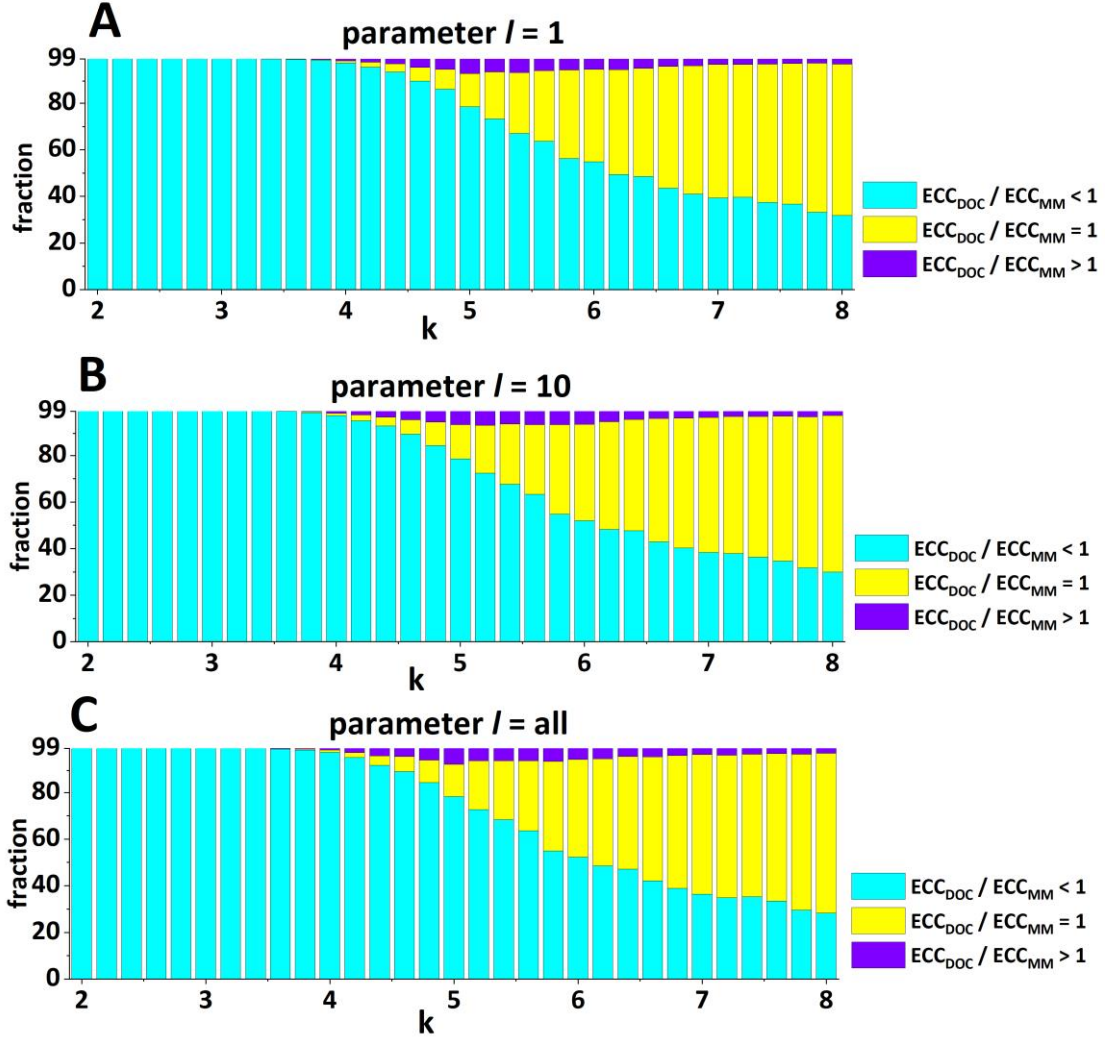


Figure 7. Performance of the DOC algorithm on temporal subgraphs when $l=1$, 10 and all . (A) - (C) The performance of the DOC algorithm on the temporal subgraph with different parameters l . The horizontal axis represents the average degree k of the network. For any given average degree k , the fraction is computed based on the average fraction of all temporal subgraphs with different change rates r .

4.3 Results of real dynamic networks

We performed a performance analysis of the DOC algorithm on 20 real-world networks. This was because the dynamic networks generated by the ER random network model undergo a completely random change process, which makes it challenging to anticipate changes in the network structure.

First, we calculated the overall ECC for each of the 20 real networks and presented the results in Table 1. We compared the ECC of *DOC* and *MM* algorithm, where lower values indicate better performance. Our analysis revealed that the DOC algorithm consistently outperformed the MM algorithm, with an average ECC_{DOC}/ECC_{MM} of 0.81 across all networks. Among the 20 networks, the email-Eu-core-temporal network had the highest performance, achieving $ECC_{DOC}/ECC_{MM}=0.50$, while the sx-superuser-a2q and sx-superuser-c2q networks had the lowest performance, both with $ECC_{DOC}/ECC_{MM}=0.99$ (Table 1).

We further conducted a detailed analysis about the performance of the DOC algorithm on real networks, using a similar strategy as that used for synthetic networks (Figures 8 and 9). In Figure 8, we present the fraction of different ECC optimization efficiencies (ECC_{DOC}/ECC_{MM}) for all temporal subgraphs in each network, while Figure 9 provides a more detailed view of the results for each temporal subgraph. Our analysis revealed significant performance fluctuations of the DOC algorithm across different temporal subgraphs, even within the same real dynamic network (Figure 9). We attribute this phenomenon to the fact that different temporal subgraphs within the same real network exhibit varying change rates (or similarities), while in synthetic network experiments, the change rate for temporal subgraphs within the same dynamic network is fixed. To investigate this phenomenon, we employed the *node similarity* $_i = \frac{|v_{i-1} \cap v_i|}{|v_{i-1} \cup v_i|}$ metric to quantify the node similarity between neighboring temporal subgraphs, and the *edge similarity* $_i = \frac{|E_{i-1} \cap E_i|}{|E_{i-1} \cup E_i|}$ metric to measure the structural similarity between adjacent neighboring subgraphs. Here, v_i and E_i represent the node set and edge set of temporal subgraphs G_i , respectively.

The results indicate that the node similarity and edge similarity of neighboring temporal subgraphs have a significant impact on the optimization efficiency of the DOC algorithm. Networks with higher edge similarity and node similarity tend to have lower ECC_{DOC}/ECC_{MM} (Figure 10). For the top five networks with the best ECC optimized performance, the mean ECC_{DOC}/ECC_{MM} is 0.54, while the mean node similarity is 0.87, and the mean edge similarity is 0.45 (Table 1). On the other hand, the worst five networks in terms of ECC optimized performance have a mean ECC_{DOC}/ECC_{MM} of 0.99, while the mean node similarity is 0.17, and a mean edge similarity is only 0.03 (Table 1).

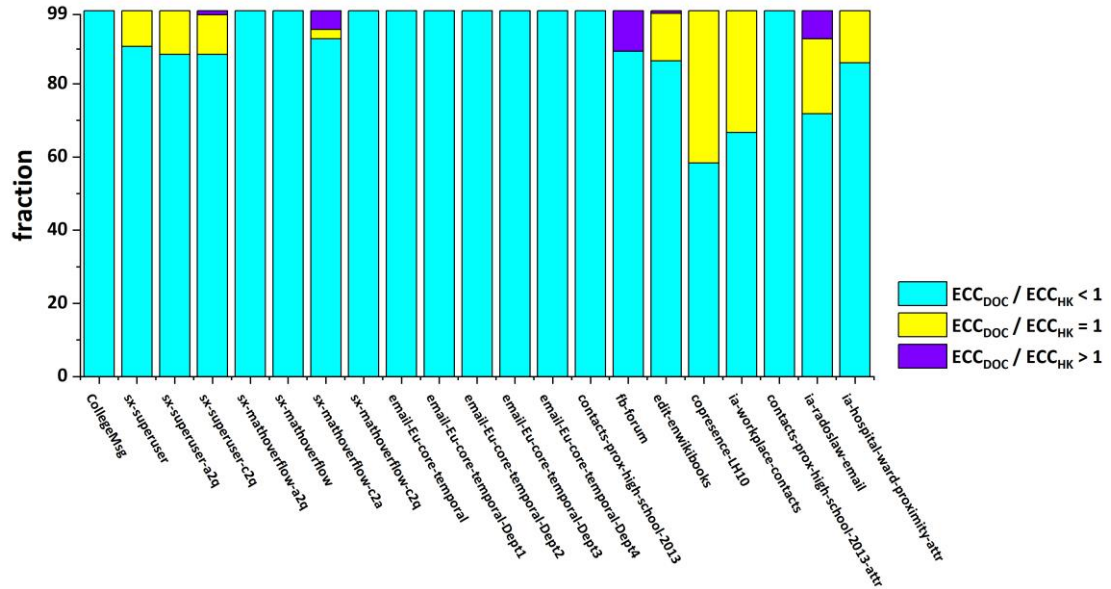


Figure 8. Performance of the DOC algorithm on temporal subgraphs in real network. The horizontal axis represents different real networks, and the vertical axis represents the temporal subgraph ratio.

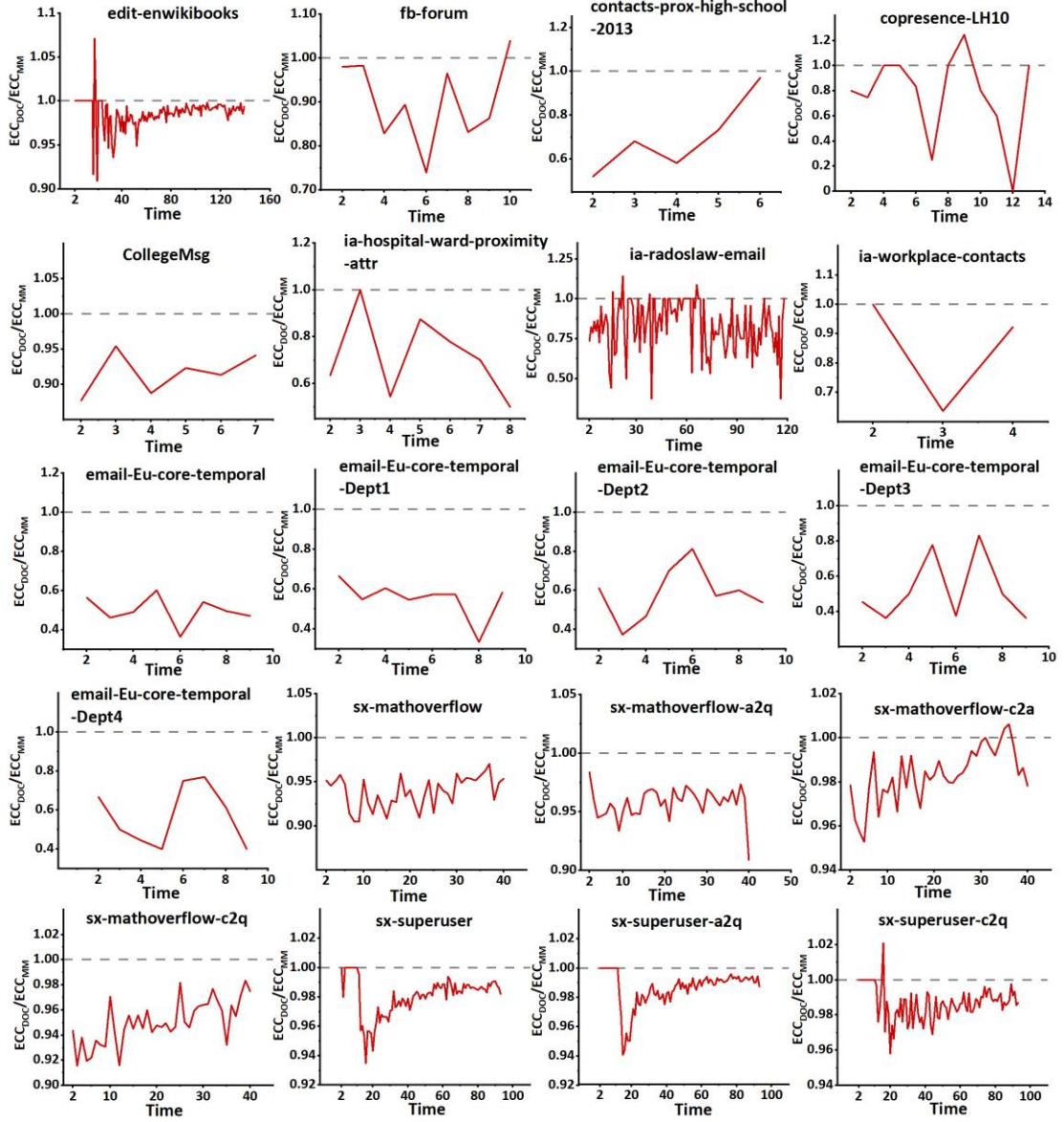


Figure 9. Optimization of the ECC for each temporal subgraphs in real networks. The horizontal-axis represents the temporal subgraphs at different time points, while the vertical-axis represents the ECC ratios of the two algorithms. The gray dashed line with $y=1$ serves as the baseline, where the region above the line indicates that $ECC_{DOC}/ECC_{MM} > 1$, indicating the occurrence of negative optimization.

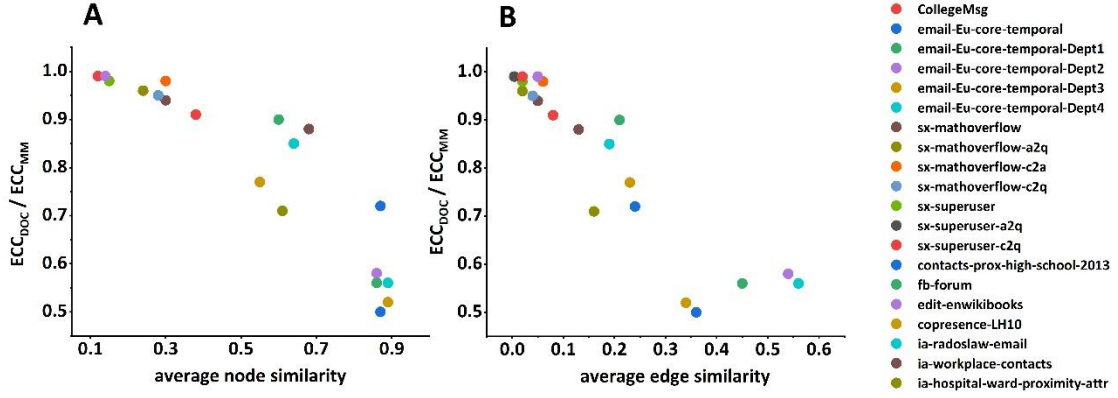


Figure 10. Relationship between ECC optimization efficiency and similarity of temporal subgraphs in real networks. **(A)** The relationship between the average node similarity and the ECC optimization efficiency. **(B)** The relationship between the average edge similarity and the ECC optimization efficiency. The smaller ECC_{DOC}/ECC_{MM} means the higher ECC optimization efficiency.

TABLE 1. Real networks results. N is the number of nodes of the network; K is the average degree of the network; τ is the temporal subgraph split length (unix timestamp); T is the number of temporal subgraphs contained in that dynamic network; S_n and S_e denote the node and edge similarity of the network, respectively.

ECC_{DOC}	ECC_{MM}	ECC_{DOC}/ECC_{MM}	$UMDS_{DOC}$	$UMDS_{MM}$	$UMDS_{DOC}/UMDS_{MM}$
934	1023	0.91	1158	1211	0.96
406	811	0.5	443	587	0.75
154	275	0.56	171	201	0.85
68	117	0.58	69	92	0.75
43	82	0.52	40	52	0.77
55	99	0.56	62	83	0.75
21508	22919	0.94	13311	13275	1
24279	25320	0.96	15880	15351	1.03
18246	18536	0.98	10851	10832	1
12018	12634	0.95	6372	6423	0.99
207738	211540	0.98	135055	130403	1.04
189038	191514	0.99	137009	131976	1.04
67131	68091	0.99	45416	43773	1.04
96	134	0.72	120	135	0.89
815	908	0.9	754	774	0.97
334285	337951	0.99	127876	126508	1.01
33	43	0.77	25	31	0.81
1706	2017	0.85	166	165	1.01
37	42	0.88	42	47	0.89
45	63	0.71	45	52	0.87

Dynamic Networks	N (mean/range)	K (mean/range)	τ	T	S _n (mean/range)	S _e (mean/range)	Average number of MDS
CollegeMsg	631.86/200-1371	7.35/2.37-15.012	2592000	7	0.38/0.29-0.45	0.08/0.03-0.11	236.71
email-Eu-core-temporal	763.22/738-818	19.62/17.79-21.93	5184000	9	0.87/0.84-0.89	0.36/0.34-0.38	148.33
email-Eu-core-temporal-Dept1	231.67/219-239	9.94/8.81-11.99	5184000	9	0.86/0.84-0.88	0.45/0.43-0.48	55.78
email-Eu-core-temporal-Dept2	120.78/115-127	13.28/11.57-14.55	5184000	9	0.86/0.84-0.89	0.54/0.50-0.58	20.11
email-Eu-core-temporal-Dept3	72.67/66-81	11.94/10.32-13.56	5184000	9	0.89/0.85-0.95	0.34/0.28-0.39	13.78
email-Eu-core-temporal-Dept4	108.11/102-120	11.36/9.44-12.63	5184000	9	0.89/0.85-0.93	0.56/0.47-0.60	16.44
sx-mathoverflow	2038.02/812-2461	7.93/3.46-14.77	5184000	40	0.30/0.19-0.37	0.05/0.03-0.07	694
sx-mathoverflow-a2q	1532.75/403-1866	3.36/1.48-8.49	5184000	40	0.24/0.11-0.31	0.02/0.004-0.03	874.1
sx-mathoverflow-c2a	1185.18/356-1433	4.71/2.10-9.26	5184000	40	0.30/0.17-0.37	0.06/0.03-0.08	578.9
sx-mathoverflow-c2q	1285.4/384-1628	5.01/2.90-7.45	5184000	40	0.28/0.17-0.33	0.04/0.02-0.05	498
sx-superuser	5642.14/39-10246	4.07/1.6-10.24	2592000	93	0.15/0.01-0.35	0.02/0-0.03	2496.41
sx-superuser-a2q	4032.52/19-6429	2.33/1.26-6.23	2592000	93	0.12/0.01-0.31	0.004/0-0.02	2385.38
sx-superuser-c2q	2171.78/2-4352	3.04/1-3.71	2592000	93	0.12/0-0.24	0.02/0-0.05	927.6
contacts-prox-high-school-2013	291.33/232-312	12.90/5.68-16.6	70000	6	0.87/0.77-0.91	0.24/0.16-0.29	52.5
fb-forum	434.5/109-728	4.86/2.11-12.59	1500000	10	0.60/0.25-0.76	0.21/0.1-0.28	212.6
edit-enwikibooks	3453.56/2-14451	1.97/1-2.48	2000000	139	0.14/0-0.33	0.05/0-0.3	2962.58
copresence-LH10	31.54/10-48	15.32/3.4-26.65	20000	13	0.55/0.29-0.74	0.23/0.06-0.48	4.85
ia-radostlaw-email	93.94/2-140	7.64/1.0-14.89	200000	118	0.64/0.01-1	0.19/0-0.32	22.22
ia-workplace-contacts	73.75/62-87	6.82/3.03-10.94	300000	4	0.68/0.65-0.74	0.13/0.11-0.13	20
ia-hospital-ward-proximity-attr	42/32-49	12.56/6.94-17.49	48000	8	0.61/0.51-0.75	0.16/0.07-0.37	15.5

5.4 Algorithm Bounds

In our results, when the rate of network variation is low (or the similarity is high), the DOC algorithm effectively reduces the ECC of both synthesized and real dynamic networks (Figure 5, 6, 7 and 10). However, when the network changes extremely, i.e., the change rate between adjacent temporal subgraphs is high, the algorithm performance will decrease significantly (Figure 10).

This is because the drastic change of the network renders the weights set in advance ineffective, which leads to the ECC results of the DOC algorithm being equal to or even worse than those of the MM algorithm. Figure 11 illustrates two extreme cases of temporal subgraphs.

For temporal subgraph G_i , assuming the MDS calculated by the DOC algorithm is $\{1,3,5\}$, and the MDS calculated by the MM algorithm is $\{1,4,6\}$ (Figure 11A). After the temporal subgraph switches from G_i to G_{i+1} (Figure 11B), the MDS obtained by both the MM algorithm and the DOC algorithm is the same, i.e., $\{4, 6, 7, 8\}$. However, $ECC_{i+1,MM}=2$ is less than $ECC_{i+1,DOC}=4$, indicating that the DOC algorithm has lower performance and produces a larger ECC. In another case, when the temporal subgraph switches from G_i to $G_{i+1'}$ (Figure 11C), the MDS obtained by both the MM algorithm and the DOC algorithm is $\{2, 7, 8\}$. In this case, the ECC result of the two algorithms is same, and the $ECC_{i+1',DOC}=ECC_{i+1',MM}=3$. In Figure 11, the change rate of the temporal subgraphs is extremely high, approaching 1.00. However, in the synthetic dynamic network (random network model), once the network change rate exceeds 0.50, the performance of the DOC algorithm is almost the same as that of the MM algorithm.

To elaborate further, in networks with extreme changes, the performance of the DOC algorithm has a lower limit that is equivalent to that of the MM algorithm, instead of continuously decreasing with the growth of the change rate. This is because, in the MM algorithm, the search for augmenting paths is conducted in a default or random order, which is unbiased. When the weights in the DOC algorithm become ineffective, the DOC algorithm will behave the same as the MM algorithm and perform matching in the default order. In this scenario, even if there is a slight discrepancy in the ECC results of the two algorithms in a single temporal subgraph, the overall ECC of the dynamic network will be very similar.

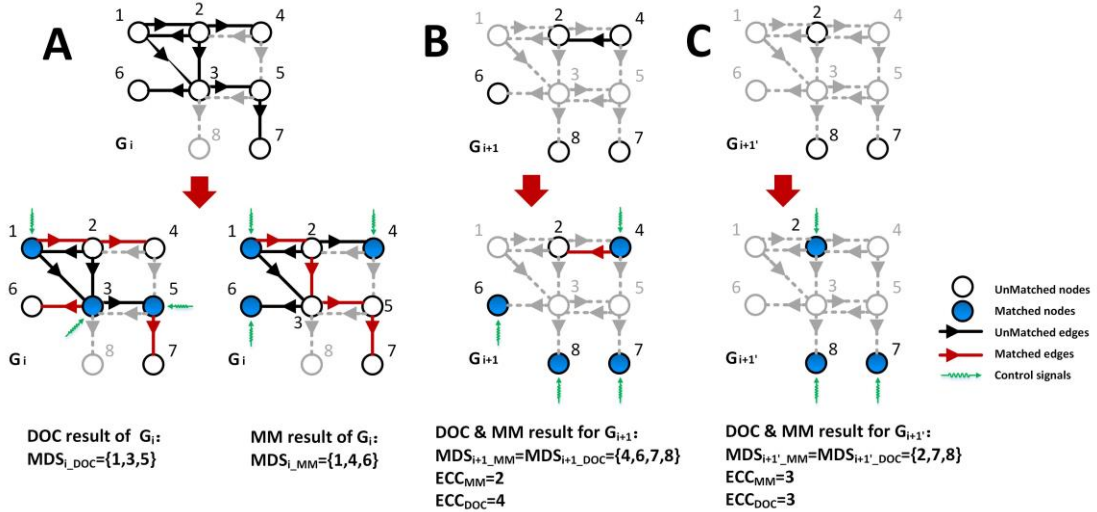


Figure 11. Examples of extreme temporal subgraph variations. (A) A temporal subgraph G_i , with the MDS calculated by the DOC and MM algorithms being $\{1, 3, 5\}$ and $\{1, 4, 6\}$, respectively. (B) Temporal subgraph G_{i+1} , where the MM algorithm outperforms the DOC algorithm in terms of ECC optimization efficiency. (C) Temporal subgraph $G_{i+1'}$, where the DOC algorithm is equally efficient as the MM algorithm in terms of ECC optimization efficiency.

5. Conclusion

Real-time dynamic networks can be represented as a sequence of static temporal subgraphs, and the MDS of these subgraphs undergoes significant variation due to changes in the

subgraphs's topological structure over time. However, it is challenging to anticipate these changes in advance for most real-time dynamic networks. In this study, we proposed an optimization method for selecting control schemes for dynamic networks in real-time. We assigned weights to each node in the current temporal subgraph based on the MDS of the previous time steps and the network's topological structure. We then improved the maximum matching algorithm using these weights to find more stable and centralized control schemes. Our algorithm was evaluated on both synthetic and real networks, and the results demonstrated that the similarity of the temporal subgraphs has a direct impact on the performance of the DOC algorithm. Specifically, DOC achieved significant optimization effects at higher levels of similarity. We further discussed the bounds of the DOC algorithm and found that in cases of extreme variations in the network, the performance of the DOC algorithm may be equal to or worse than that of the MM algorithm. Overall, in most normal cases of real-time dynamic networks, the DOC algorithm outperforms the MM algorithm.

Author contribution

XZ is the corresponding author. XZ conceived the study, drafted and revised the manuscript. CP and CZ implemented the algorithm, performed data analysis, preparing the figures and drafted the manuscript. ZS collated the data and revised the figures. All authors contributed substantially to the preparation of the manuscript.

Acknowledgment

This paper is supported by National Natural Science Foundation of China [62176129], National Key Research and Development Program [2022YFC2405603] of Ministry of Science and Technology of China, Jiangsu Provincial Key Research and Development Program [BE2021617] of Science and Technology Department of Jiangsu Province, the Key Project of the National Natural Science Foundation of China [U1908212], Central government guided local science and Technology Development Fund Project [1653137155953], Liaoning Province "takes the lead" science and technology research project [2021jh1/10400006] and the General project of Liaoning Provincial Department of Education [LJKMZ20220613].

Reference

- [1] Kalman and E. R., "Mathematical Description of Linear Dynamical Systems," *Journal of the Society for Industrial*, vol. 1, no. 2, pp. 152-192, 1963.
- [2] Y. Y. Liu, J. J. Slotine, and A. L. Barabasi, "Controllability of complex networks," *Nature*, vol. 473, no. 7346, pp. 167-73, May 12 2011.
- [3] C. T. Lin, "Structural controllability," *IEEE Transactions on Automatic Control*, vol. 19, no. 3, pp. 201-208, 1974.
- [4] D. J. Watts and S. H. Strogatz, "Collective dynamics of 'small-world' networks," *Nature*, vol. 393, no. 6684, pp. 440-2, Jun 4 1998.
- [5] S. Wuchty, "Controllability in protein interaction networks," *Proc Natl Acad Sci U S A*, vol. 111, no. 19, pp. 7156-60, May 13 2014.
- [6] X. Liu and L. Pan, "Identifying Driver Nodes in the Human Signaling Network Using Structural Controllability Analysis," *IEEE/ACM Trans Comput Biol Bioinform*, vol. 12, no. 2, pp. 467-72, Mar-Apr 2015.
- [7] A. Kumar, I. Vlachos, A. Aertsen, and C. Boucsein, "Challenges of understanding brain function

- by selective modulation of neuronal subpopulations," *Trends Neurosci*, vol. 36, no. 10, pp. 579-86, Oct 2013.
- [8] A. Vinayagam *et al.*, "Controllability analysis of the directed human protein interaction network identifies disease genes and drug targets," *Proc Natl Acad Sci U S A*, vol. 113, no. 18, pp. 4976-81, May 3 2016.
 - [9] L. Wu, Y. Shen, M. Li, and F. X. Wu, "Network output controllability-based method for drug target identification," *IEEE Trans Nanobioscience*, vol. 14, no. 2, pp. 184-91, Mar 2015.
 - [10] C. Pan *et al.*, "Control Analysis of Protein-Protein Interaction Network Reveals Potential Regulatory Targets for MYCN," *Front Oncol*, vol. 11, p. 633579, 2021.
 - [11] Z. Xizhe, "Altering indispensable proteins in controlling directed human protein interaction network," *IEEE/ACM Transactions on Computational Biology Bioinformatics*, pp. 1-1, 2018.
 - [12] S. Gu *et al.*, "Controllability of structural brain networks," *Nat Commun*, vol. 6, p. 8414, Oct 1 2015.
 - [13] S. F. Muldoon *et al.*, "Stimulation-Based Control of Dynamic Brain Networks," *PLoS Comput Biol*, vol. 12, no. 9, p. e1005076, Sep 2016, Art. no. e1005076.
 - [14] E. Tang and D. S. Bassett, "Colloquium: Control of dynamics in brain networks," *Reviews of Modern Physics*, vol. 90, no. 3, Aug 14 2018, Art. no. 031003.
 - [15] D. Delpini, S. Battiston, M. Riccaboni, G. Gabbi, F. Pammolli, and G. Caldarelli, "Evolution of controllability in interbank networks," *Sci Rep*, vol. 3, p. 1626, Apr 9 2013, Art. no. 1626.
 - [16] R. M. Razakanirina and B. Chopard, "Risk analysis and controllability of credit market," *ESAIM: Proc.*, vol. 49, pp. 91-101, 2015.
 - [17] Paul, Glasserman, H., Peyton, and Young, "How likely is contagion in financial networks?," *Journal of Banking Finance*, 2015.
 - [18] N. Chen, X. Liu, and D. D. Yao, "An Optimization View of Financial Systemic Risk Modeling: Network Effect and Market Liquidity Effect," *Socence Electronic Publishing*, 2016.
 - [19] S. Poledna and S. Thurner, "Elimination of systemic risk in financial networks by means of a systemic risk transaction tax," *Quantitative Finance*, vol. 16, no. 10, pp. 1599-1613, 2016 2016.
 - [20] Y.-Y. Liu and A.-L. Barabási, "Control principles of complex systems," *Reviews of Modern Physics*, vol. 88, no. 3, Sep 6 2016, Art. no. 035006.
 - [21] J. Ruths and D. Ruths, "Control Profiles of Complex Networks," *Science*, vol. 343, no. 6177, pp. 1373-6, 2014.
 - [22] C. Campbell, J. Ruths, D. Ruths, K. Shea, and R. Albert, "Topological constraints on network control profiles," *Sci Rep*, vol. 5, no. 1, p. 18693, Dec 22 2015.
 - [23] J. Gao, Y. Y. Liu, R. M. D'Souza, and A. L. Barabasi, "Target control of complex networks," *Nat Commun*, vol. 5, no. 1, p. 5415, Nov 12 2014.
 - [24] Z. Yuan, C. Zhao, Z. Di, W. X. Wang, and Y. C. Lai, "Exact controllability of complex networks," *Nat Commun*, vol. 4, no. 1, p. 2447, 2013/09/12 2013.
 - [25] X. Zhang, H. Wang, and T. Lv, "Efficient target control of complex networks based on preferential matching," *PLoS One*, vol. 12, no. 4, p. e0175375, 2017.
 - [26] X. Zhang, T. Lv, X. Yang, and B. Zhang, "Structural controllability of complex networks based on preferential matching," *PLoS One*, vol. 9, no. 11, p. e112039, Nov 6 2014, Art. no. e112039.
 - [27] X. Zhang, Y. Zhu, and Y. Zhao, "Altering control modes of complex networks by reversing edges," *Physica A: Statistical Mechanics its Applications*, vol. 561, no. C, p. 125249, 2021.
 - [28] X. Zhang and Q. Li, "Altering control modes of complex networks based on edge removal,"

Physica A: Statistical Mechanics and its Applications, vol. 516, 2019.

- [29] P. Panzarasa, T. Opsahl, and K. M. Carley, "Patterns and dynamics of users' behavior and interaction: Network analysis of an online community," *Journal of the American Society for Information Science and Technology*, vol. 60, no. 5, pp. 911-932, May 2009.
- [30] A. Li, S. P. Cornelius, Y. Y. Liu, L. Wang, and A. L. Barabasi, "The fundamental advantages of temporal networks," *Science*, vol. 358, no. 6366, pp. 1042-1046, Nov 24 2017.
- [31] Y. Cui, S. He, M. Wu, C. Zhou, and J. Chen, "Improving the Controllability of Complex Networks by Temporal Segmentation," *IEEE Transactions on Network Science Engineering*, vol. PP, no. 99, pp. 1-1, 2020.
- [32] B. Hou, X. Li, and G. Chen, "Structural Controllability of Temporally Switching Networks," *IEEE Transactions on Circuits and Systems I: Regular Papers*, vol. 63, no. 10, pp. 1771-1781, Oct 2016.
- [33] M. Pósfai and P. Hövel, "Structural controllability of temporal networks," *New Journal of Physics*, vol. 16, no. 12, Dec 22 2014, Art. no. 123055.
- [34] F. M. Babak Ravandi, John A Springer "Identifying and using driver nodes in temporal networks," *Journal of Complex Networks*, vol. Volume 8, Issue 2, April 2020, cnz025, 2019.
- [35] L. G. Valiant, "The complexity of computing the permanent," *Theoretical Computer Science*, vol. 8, no. 2, pp. 189-201, 1979.
- [36] X. Zhang, T. Lv, and Y. Pu, "Input graph: the hidden geometry in controlling complex networks," *Sci Rep*, vol. 6, p. 38209, Nov 30 2016, Art. no. 38209.
- [37] X. Zhang, J. Han, and W. Zhang, "An efficient algorithm for finding all possible input nodes for controlling complex networks," *Scientific Reports*, no. 1, 2017.
- [38] L. E. C. Rocha, N. Masuda, and P. Holme, "Sampling of temporal networks: Methods and biases," *Phys Rev E*, vol. 96, no. 5-1, p. 052302, Nov 2017.
- [39] E. Almaas, B. Kovacs, T. Vicsek, Z. N. Oltvai, and A. L. Barabasi, "Global organization of metabolic fluxes in the bacterium *Escherichia coli*," (in eng), *Nature*, vol. 427, no. 6977, pp. 839-43, Feb 26 2004.
- [40] P. Holme and J. Saramäki, "Temporal networks," *Physics Reports*, vol. 519, no. 3, pp. 97-125, 2012/10/01/ 2012.
- [41] W. C. Salmon, *Zeno's paradoxes*. Hackett Publishing, 2001.
- [42] J. Zhang, K. H. Johansson, J. Lygeros, and S. Sastry, "Zeno hybrid systems," *International Journal of Robust and Nonlinear Control*, <https://doi.org/10.1002/rnc.592> vol. 11, no. 5, pp. 435-451, 2001/04/30 2001.
- [43] Y. Pan and X. Li, "Structural controllability and controlling centrality of temporal networks," *PLoS One*, vol. 9, no. 4, p. e94998, Apr 18 2014, Art. no. e94998.
- [44] K. Murota, "Matrices and matroids for systems analysis," *algorithms combinatorics*, vol. 20, no. 1, pp. 6-10, 2008.
- [45] J. E. Hopcroft and R. M. Karp, "An $n^{5/2}$ Algorithm for Maximum Matchings in Bipartite Graphs," vol. 2, no. 4, pp. 225-231, 1973.
- [46] L. Zdeborová and M. Mézard, "The number of matchings in random graphs," *Journal of Statistical Mechanics: Theory and Experiment*, vol. 2006, no. 05, pp. P05003-P05003, 2006.
- [47] T. Jia and A. L. Barabasi, "Control capacity and a random sampling method in exploring controllability of complex networks," *Sci Rep*, vol. 3, p. 2354, 2013.
- [48] A. L. Barabasi and R. E. Crandall, "Linked: The New Science of Networks," *American Journal of Physics*, vol. 71, no. 4, pp. 243-270, 2002.

- [49] R. Albert and A.-L. Barabási, "Statistical mechanics of complex networks," *Reviews of Modern Physics*, vol. 74, no. 1, pp. 47-97, 01/30/ 2002.
- [50] V. Martínez, F. Berzal, and J. C. Cubero, "A Survey of Link Prediction in Complex Networks," *Acm Computing Surveys*, vol. 49, no. 4, p. 69, 2016.
- [51] A. L. Barabasi and R. Albert, "Emergence of scaling in random networks," *Science*, vol. 286, no. 5439, pp. 509-12, Oct 15 1999.
- [52] A. Paranjape and A. R. Benson, *Motifs in Temporal Networks* (Wsdm'17: Proceedings of the Tenth Acm International Conference on Web Search and Data Mining). 2017, pp. 601-610.
- [53] R. Rossi and N. Ahmed, "The network data repository with interactive graph analytics and visualization," in *Twenty-ninth AAAI conference on artificial intelligence*, 2015.